# Ballistic Frenkel-exciton gate with a high on-off ratio

Aaron Sup [1], Bernard Yurke [2,*] and Richard Elliott [2]
[1]*Department of Physics, Boise State University, Boise, Idaho 83725, USA*
[2]*Micron School of Materials Science and Engineering, Boise State University, Boise, Idaho 83706, USA*

(Received 5 April 2024; accepted 3 July 2024; published 22 August 2024)

Here it is shown that the exciton interactions within organic dye aggregates, as modeled by the Frenkel Hamiltonian, enable the construction of an on-off switchable exciton gate. In this construction, a single exciton residing on a controlling gate molecule may pass or inhibit the ballistic propagation of an exciton in a proximal gate channel consisting of an array of dye molecules. High on-off ratios in excess of $10^2$ can be achieved through the use of static difference dipole-dipole interactions between the gate and the gate channel which effectively creates a switchable Bragg grating. The gate channel and controlling gate molecule exhibit entanglement with the quantum-mechanical superposition of the presence and absence of exciton occupation on the gate molecule.

DOI: 10.1103/PhysRevA.110.022616

## I. INTRODUCTION

In an aggregate of densely packed organic dye molecules, the excitation resulting from the transition of a dye molecule from the singlet ground state $S_0$ to the singlet excited state $S_1$ behaves as a particle that can propagate throughout the aggregate in a quantum-mechanical wavelike manner. This quasiparticle is referred to as a Frenkel exciton [1]. Its coherent transfer between molecules is mediated by the dipole-dipole coupling of transition dipoles between pairs of dye molecules. Frenkel excitons can also exhibit two-particle interactions. The two-particle interaction between excitons residing on separate dyes arises from the change in the static charge distribution resulting from the $S_0$ to the $S_1$ molecular transition. For asymmetric molecules the dipole component of the electric field of the static charge distribution may be dominant. In that case the exciton-exciton interaction has the form of a dipole-dipole interaction for which the dipoles are the difference between the excited-state and ground-state dipoles [1]. We refer to these as difference static dipoles [2,3]. A two-particle interaction also arises when two excitons reside on the same dye [4,5], that is, when the dye is excited to a singlet state $S_n$ having a higher energy than the singlet state $S_1$. The strength of this interaction is the energy cost of double occupancy. Frenkel-exciton theory models well the coherent transfer of excitons between dyes and the interdye and intradye exciton-exciton interactions, succinctly describing the exciton dynamics of dye aggregates when the coupling of these excitons with molecular vibrations can be neglected. In addition, it is a very useful tool when considering processes that are fast compared to the exciton dephasing time.

The Frenkel model belongs to a class of models in which a complete set of gates for scalable universal quantum computation can be realized [6–8]. Frenkel excitons are thus attractive candidates for applications in quantum information processing. They are also attractive candidates for ultrafast switching and information processing applications. The switching speed of these gates is set by the transition dipole-dipole interaction energy and by the exciton-exciton interaction energy. The strength of both of these interactions can be in the 100-eV range [3,9,10], thereby enabling switching on a 10-fs timescale with possible room-temperature operation. Due to these desirable features, the design of exciton-based gates for quantum computing [11–13] and for switching [14] has received considerable attention. Although the concern here is with systems employing optical transitions between the singlet ground state and first singlet excited state typical of organic dyes, we note that systems employing singlet fission and triplet annihilation have also received attention for information processing applications [15].

Here we present a gate that controls the ballistic propagation of excitons through a gate channel via static difference dipole interactions between the gate and channel. Through these interactions, a compact switchable excitonic Bragg grating is implemented that enables the gate to achieve a high on-off ratio. The device is depicted in Fig. 1. Two attached linear arrays of dye molecules serve as transmission lines along which an exciton can propagate ballistically, that is, without loss of energy. They attach to the left and right of the gate, as shown, and one provides a source channel of excitons as input to the gate and if permitted by the gate may propagate through to a second transmission line referred to as the drain. The gate is referred to as off when transmission to the drain is highly suppressed. As shown, the gate consists of a single control molecule C and the gate channel consists of a short array of dye molecules wrapped around the gate molecule. The excitons are to be prepared on the source side of the gate (and read on the drain side) by antennas attached to the transmission line, which convert photons into excitons (and vice versa). These antennas are tailored to couple to a desired polarization; therefore the gate, source, and drain can be independently excited.

[*]Also at Department of Electrical and Computer Engineering, Boise State University, Boise, Idaho, USA.

 

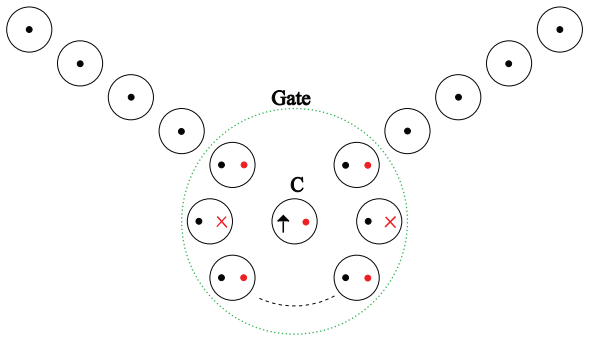


FIG. 1. Schematic representation of the aggregate structure of the Frenkel-exciton gate. Here the black circles represent dye molecules which interact via nearest-neighbor dipole interactions. The interior black symbols represent the transition dipoles, with dots representing dipoles directed out of the page. The red marks represent the static difference dipoles, with dots representing dipoles directed out of the page and the crosses representing dipoles directed into the page. The gate region of the device is marked by the green dotted circle, with the controlling gate molecule marked with a C.

As configured, the gate molecule C and gate-channel molecules interact only through the exciton-exciton interactions afforded by different static dipole interactions. Interactions between the gate molecule and gate channel via the transition dipole-dipole interaction are suppressed by orienting the transition dipole of the gate molecule to be orthogonal to the transition dipoles of the gate-channel molecules. Such an arrangement is depicted in Fig. 1 where the transition dipole of the gate molecule lies in the plane of the figure, while all the other transition dipoles are orthogonal to the figure plane. This prevents a gate exciton from hopping onto the gate channel or a gate-channel exciton from hopping onto the gate. That the molecules can be arranged to set the transition dipole-dipole coupling between the gate and the gate channel to zero without simultaneously causing the difference static dipole coupling to vanish is possible due to the existence of dye molecules for which the transition dipole and the static difference dipole are not parallel [9]. In the system shown in Fig. 1, this is achieved by employing a gate molecule for which the transition dipole and the static difference dipole are orthogonal, while for the gate-channel molecules the transition dipole and static difference dipoles are parallel. The input and output transmission-line channels may be constructed of symmetric molecules for which there is no difference static dipole.

The availability of dyes with differing static difference dipole moments also enables the construction of gate channels for which the exciton-exciton couplings between the gate molecule and the gate-channel molecules are not all the same. In particular, the coupling strengths can be modulated in magnitude or sign such that an exciton in the gate channel experiences a periodic potential when an exciton resides on the gate molecule. In the system depicted in Fig. 1, this is simply accomplished by choosing successive molecules in the gate channel to be aligned in an antiparallel manner. In the absence of an exciton on the gate molecule, this periodic potential is absent. In this manner an on-off switchable Bragg grating is implemented. If the Bragg grating has a periodicity of 2 compared to the spacing between neighboring dyes, the grating will open a band gap at the center of the channel band for a grating of infinite extent, thereby blocking exciton passage through the gate channel when their energy lies within this band gap. The width of this band gap is proportional to the amplitude of the periodic modulation of the exciton-exciton interaction energy. For a grating of finite length, the blockage will not be complete. For a gate channel wrapped around a gate molecule, the length of the grating is limited to about 2.5 periods. However, we show that even such a short grating is effective in suppressing exciton transmission through the gate channel, thereby enabling on-off ratios in excess of $10^2$.

This gate provides a means for generating quantum-mechanical states in which the gate subsystem becomes entangled with the channel subsystem. At the level of approximation we have employed, the system is energy conserving and the exciton-exciton coupling between the gate and channel molecules is number conserving: The number of excitons on the gate molecule is fixed. Thus, for a system prepared with the gate molecule in a superposition state with an exciton present or absent, the gate remains in that superposition as long as no measurement is performed to collapse it. The incoming channel exciton, upon interacting with the gate, will then be put into a superposition of states consisting of passing through and reflecting off of the gate, thereby entangling the gate with an exciton heading rightward or leftward down the attached transmission lines.

Prior to considering the operation of the gate, a couple of limitations are worthy of mention. First, the analysis below neglects exciton-vibration coupling that causes exciton dephasing in real aggregate systems. Hence, the analysis applies for cases when exciton switching is carried out on a timescale that is fast compared to the exciton dephasing time, which at cryogenic temperatures can be in the $10^2$-fs range [16]. Second, it is desirable to consider the operation of this gate as a transistor in which the gate molecule controls the flow of a large number of excitons in the gate channel. This extension of the analysis below is also made difficult because of the exciton-exciton interactions that can occur when more than one exciton resides in the gate channel. The analysis of such a gate then becomes a complex many-body problem, which we have not attempted to solve.

## II. HAMILTONIAN

In order to avoid dealing with the complex many-body problem that results if multiple excitons reside in the gate channel and/or on the input and output exciton transmission lines, our analysis is restricted to the case when at most one exciton resides on the gate-channel–transmission-line system and at most one exciton resides on the gate molecule. For systems such as this, which have been rigged to prevent exciton double occupancy, the Hamiltonian has the form [1]

$$H = \sum_n E_n a_n^\dagger a_n + \sum_{n,m} J_{n,m}(a_n^\dagger a_m + a_m^\dagger a_n) + \sum_{n,m} K_{n,m}(a_n^\dagger a_m^\dagger a_n a_m), \quad (1)$$

where $a_n$ is the annihilation operator for an exciton at a site $n$ on the aggregate. The annihilation operators satisfy the usual boson commutation relations

$$[a_n, a_m] = 0 \tag{2}$$

and

$$[a_n, a_m^\dagger] = \delta_{n,m}. \tag{3}$$

The transition energy $E_n$ is the energy required to optically excite a chromophore at site $n$ into its first excited state. The energy $J_{n,m}$ will be referred to as the hopping energy and is modeled as a dipole-dipole interaction [1] between the transition dipoles of the chromophores at sites $n$ and $m$,

$$J_{n,m} = \frac{\mu_n \mu_m}{4\pi\epsilon R^3}[\mathbf{n}_n \cdot \mathbf{n}_m - 3(\mathbf{n}_{n,m} \cdot \mathbf{n}_n)(\mathbf{n}_{n,m} \cdot \mathbf{n}_m)], \tag{4}$$

where $\mathbf{n}_n$ is the unit vector representing the direction of the dipole moment whose magnitude $\mu_n$ is the dipole moment, $R$ is the separation distance between the chromophores at sites $n$ and $m$, and $\mathbf{n}_{n,m}$ represents the unit vector whose direction points from the center of chromophore $n$ to the center of chromophore $m$. Thus, by designing the orientations and distance between the chromophores in an aggregate, one can engineer the hopping energies (frequencies) to have a particular desired value. Here $K_{n,m}$ is the exciton-exciton interaction energy between an exciton residing on chromophore $n$ and another exciton residing on chromophore $m$. This interaction is modeled by considering the difference static dipoles whose magnitude at site $n$ is $d_n$ and whose unit orientation vector is $\mathbf{m}_n$. Thus the interaction energy is the dipole-dipole interaction [1]

$$K_{n,m} = \frac{d_n d_m}{4\pi\epsilon R^3}[\mathbf{m}_n \cdot \mathbf{m}_m - 3(\mathbf{n}_{n,m} \cdot \mathbf{m}_n)(\mathbf{n}_{n,m} \cdot \mathbf{m}_m)]. \tag{5}$$

By manipulating the orientation of the chromophores we can design the system to have a particular exciton-exciton interaction energy or frequency. Of particular note is that, in general,

$$\mathbf{n}_n \times \mathbf{m}_n \neq 0, \tag{6}$$

meaning we have the freedom to manipulate $J_{n,m}$ and $K_{n,m}$ independently. This strategy is employed to engineer an aggregate configuration in which the gate-molecule dye and the gate-channel dyes have the desired $J_{m,n}$ and $K_{m,n}$ values.

## III. TRANSMISSION LINES

The exciton gate is an input-output device and as such is characterized by its scattering matrix. As a step toward the computation of the scattering matrix, we first consider exciton propagation on an exciton transmission line consisting of a one-dimensional aggregate of identical dyes [17]. From the form of the energy in Eq. (4) we see that the hopping energy decreases as the cube of the distance between the dyes; therefore, the interaction strength falls off dramatically for dyes that are anything but nearest neighbors, enabling us to first order in utilizing the nearest-neighbor approximation so that the hopping sector of the Hamiltonian (1) takes the form

$$H_J = \sum_n J_{n,n+1}(a_n^\dagger a_{n+1} + a_{n+1}^\dagger a_n). \tag{7}$$

Since we are considering the case when a single exciton resides on the gate-channel–transmission-line system, we can set $K_{m,n} = 0$ for dyes $m$ and $n$ in this system. To take advantage of translation invariance we now consider a transmission line of infinite extent in both directions. The Hamiltonian for this transmission line is given by

$$H = \sum_{n=-\infty}^{\infty} \hbar\omega_E a_n^\dagger a_n + \sum_{n=-\infty}^{\infty} \hbar\omega_J(a_n^\dagger a_m + a_m^\dagger a_n), \tag{8}$$

where $E_n = \hbar\omega_E$ and $J_{n,n+1} = \hbar\omega_J$.

The Heisenberg equations of motion for the annihilation operators are given by

$$\frac{da_n}{dt} = -i\omega_E a_n - i\omega_J(a_{n-1} + a_{n+1}) \quad \text{for } -\infty \leqslant n \leqslant \infty, \tag{9}$$

and from Bloch's theorem we can expand these solutions as Fourier modes

$$a_n = \frac{1}{\sqrt{2\pi}} \int_{-\pi}^{\pi} e^{ikn} a(k,t)dk. \tag{10}$$

Substituting this Fourier expansion into Eq. (9) and restricting our attention to the bandwidth $0 \leqslant k \leqslant \pi$, we can write our solution as the sum of an exciton pulse moving to the right and to the left,

$$a_n = \frac{1}{\sqrt{2\pi}} \int_0^{\pi} e^{-i(\omega_k t - kn)} a_+(k)dk + \frac{1}{\sqrt{2\pi}} \int_0^{\pi} e^{-i(\omega_k t + kn)} a_-(k)dk, \tag{11}$$

where the dispersion relation is

$$\omega_k = \omega_E + 2\omega_J \cos(k). \tag{12}$$

Thus we see that the exciton along a transmission line behaves as a quasiparticle propagating freely (ballistically) either to the right or to the left along the transmission line. A variety of one-exciton devices can be implemented as assemblies of transmission-line segments [17]. Given the architecture of the exciton-controlled exciton gate of Fig. 1, with the simple context and formalism of the Frenkel Hamiltonian, we next show how the gate may be implemented.

## IV. EXCITON-CONTROLLED EXCITON GATE

The device under consideration is shown in Fig. 1. The switching on-off action of this gate will be controlled by the excitation of the gate molecule C. This could be accomplished by optical pumping, for example. Note that since the transition dipole of the gate molecule is orthogonal to the transition dipoles of all other molecules, the excitation of the transmission-line–gate-channel system can be avoided with a proper choice of the optical pump pulse.

The exciton in this gate molecule will interact via the static difference dipole-dipole interaction in Eq. (5) with excitons that are moving through the gate channel, represented as a series of molecules arranged as a ring around the gate molecule in Fig. 1. Note that the transition dipole moment of the gate molecule is perpendicular to the transition dipoles of the transmission lines, and therefore excitons will not hop from the

transmission line to the control molecule. The static difference dipole moments of the molecules in the gate region also alternate in direction, which causes a periodic variation in the exciton-exciton interaction energy as the exciton propagates through the gate channel. This up-down corrugation from the alternating dipole configurations in the gate channel effectively creates a switchable Bragg grating, prompted merely by the excitation of the central, controlling gate molecule.

The number of molecules in the gate channel will be referred to as the gate size $G$. To maximize this interaction as much as possible by minimizing the distance between the gate molecule and the gate-channel molecules, we will limit the gate size to be no greater than six molecules.

Numbering the molecules of the transmission-line–gate-channel system consecutively such that the first gate-channel molecule is $n = 1$ and the last gate-channel molecule is $n = G$, we can separate the transmission lines into a source and drain, where the solution given by Eq. (11) for the source ($n \leqslant 0$) is

$$a_n = \frac{1}{\sqrt{2\pi}} \int_0^\pi e^{-i(\omega_k t - kn)} a_S^{\text{in}} dk + \frac{1}{\sqrt{2\pi}} \int_0^\pi e^{-i(\omega_k t + kn)} a_S^{\text{out}} dk \tag{13}$$

and for the drain ($n \geqslant G + 1$) is

$$a_n = \frac{1}{\sqrt{2\pi}} \int_0^\pi e^{-i(\omega_k t - kn)} a_D^{\text{out}} dk + \frac{1}{\sqrt{2\pi}} \int_0^\pi e^{-i(\omega_k t + kn)} a_D^{\text{in}} dk. \tag{14}$$

We are assuming here that for the band $0 \leqslant k \leqslant \pi$, the incoming signal in the source and the outgoing signal in the drain are moving towards positive $n$, and the outgoing signal in the source and incoming signal in the drain are moving towards negative $n$. From the dispersion relation (12) we can see that the group velocity is given by

$$v_g = -2\omega_J \sin(k) \tag{15}$$

and that such definitions can be satisfied for positive $k$ if $\omega_J$ is negative, which is realizable as can be seen in Eq. (4). This is arbitrary however, and an equivalent analysis can be carried out by reversing convention of what constitutes the incoming and outgoing signals, in which case $\omega_J$ is positive for positive $k$. We note that the transition dipoles of the transmission-line–gate-channel system molecules of Fig. 1 are aligned side by side, a configuration for which $\omega_J$ is positive.

The gate-channel molecules are arranged such that the static difference dipole-dipole interaction with the gate molecule alternates in sign for successive gate-channel molecules (see Fig. 1). This alternating increase and decrease of energy in the gate will give rise to exciton reflections and will open a band gap in between the frequencies $\omega_E - 2|\omega_J|$ and $\omega_E + 2|\omega_J|$. This band gap will be centered at a midband value of $k = \pi/2$, for which it is expected that transmission through the device will be minimized.

The Hamiltonian for the transmission-line–gate-channel system along with the gate molecule can be written as

$$H = H_S + H_D + H_G + H_J, \tag{16}$$

where $H_S$ is the Hamiltonian for the source side transmission line, $H_D$ is the Hamiltonian for the drain transmission line, $H_J$ is the hopping Hamiltonian for the entire transmission-line–gate-channel system, and $H_G$ is the Hamiltonian for the gate region. These parts of the full system Frenkel Hamiltonian are given by

$$H_S = \sum_{n=-\infty}^{0} \hbar\omega_E a_n^\dagger a_n, \tag{17}$$

$$H_D = \sum_{n=G+1}^{\infty} \hbar\omega_E a_n^\dagger a_n, \tag{18}$$

$$H_J = \sum_{n=-\infty}^{\infty} \hbar\omega_J (a_{n+1}^\dagger a_n + a_n^\dagger a_{n+1}), \tag{19}$$

and

$$H_G = \sum_{n=1}^{G} \hbar\omega_E a_n^\dagger a_n + \hbar\omega_G b^\dagger b - \sum_{n=0}^{G} (-1)^n \hbar\omega_K a_n^\dagger b^\dagger b a_n, \tag{20}$$

where $b$ is the exciton annihilation operator for the gate molecule, $\hbar\omega_G$ is the excitation energy for the gate molecule, and $\omega_K$ is defined such that $\hbar\omega_K = |K_{n,m}|$ where here the index $m$ in Eq. (5) refers to the control molecule. We adopt a configuration where $K_{m,n}$ is positive when $n$ is odd and negative when $n$ is even.

The Heisenberg equations of motion generated from the Hamiltonian (16) for the annihilation operators are

$$\frac{da_n}{dt} = -i\omega_E a_n - i\omega_J (a_{n-1} + a_{n+1}) \quad \text{for } n \leqslant 0,\ n \geqslant G+1, \tag{21}$$

$$\frac{da_n}{dt} = -i\omega_E a_n - i\omega_J (a_{n-1} + a_{n+1}) + (-1)^n i\omega_K b^\dagger b a_n \quad \text{for } 1 \leqslant n \leqslant G, \tag{22}$$

and

$$\frac{db}{dt} = -i\omega_G b + i\omega_K \sum_{n=0}^{G} (-1)^n a_n^\dagger a_n b \quad \text{for } 1 \leqslant n \leqslant G. \tag{23}$$

From Eq. (23) it is found that

$$\frac{d(b^\dagger b)}{dt} = 0 \tag{24}$$

so that $b^\dagger b = N_G$ is a constant of motion and represents the number of excitons present on the gate molecule. Since we are restricting ourselves to the case when there is at most one exciton on the gate molecule, $N_G$ is either zero or one. Equation (22) can now be written as

$$\frac{da_n}{dt} = -i[\omega_E - (-1)^n \omega_K N_G] a_n - i\omega_J (a_{n-1} + a_{n+1}) \quad \text{for } 1 \leqslant n \leqslant G. \tag{25}$$

Note that if $N_G = 0$ then Eq. (9) is recovered and an exciton transmits through the gate unimpeded.

It should be noted that, while we are treating the transmission line to be infinitely long, for which noise and decoherence

are a concern, such a treatment is for the purposes of modeling incoming and outgoing exciton pulses. The actual transmission lines in this device are envisioned to be short, making loss of coherence and noise less of a concern.

## V. TRANSMISSION THROUGH THE EXCITON GATE IN THE OFF STATE

For the exciton gate in the off state (state preventing exciton flow), $N_G = 1$, and the eigenmode solutions in the gate region ($1 \leqslant n \leqslant G$) become

$$a_n = \frac{1}{\sqrt{2\pi}} \int_0^{\pi} e^{-i\omega_k t} a_{k,n} dk, \tag{26}$$

where $a_{k,n}$ no longer have the simple form of the Bloch modes of the solutions in the source and drain transmission lines. In order to relate the values of $a_{k,n}$ to the values of $a_S^{\text{in}}$, $a_S^{\text{out}}$, $a_D^{\text{in}}$, and $a_D^{\text{out}}$, we substitute Eqs. (26), (13), and (14) into Eqs. (25) and (21) for $n$ values of 0 through $G+1$, which gives a system of equations comprised of $G+2$ equations and $G+4$ unknowns. From this system of equations we can eliminate all the values of $a_{k,1}$ through $a_{k,G}$ and express $a_D^{\text{in}}$ and $a_D^{\text{out}}$ in terms of $a_S^{\text{in}}$ and $a_S^{\text{out}}$. These relationships provide us with a transfer matrix, from which we can determine the probability that an exciton propagating along the source transmission line will continue into the drain transmission line, analogous to quantum tunneling. This tunneling probability will serve as the switching ratio of our device.

In order to simplify our system of equations we can introduce the physical parameter

$$x = \frac{\omega_K}{\omega_J}, \tag{27}$$

which we can see from Eqs. (4) and (5) defines the relative value of the transition dipole-dipole interactions of the molecules in the transmission lines to that of the difference static dipole-dipole interactions between the gate molecule and the gate-channel molecules. We then, for purposes of algebraic convenience, define the associated parameter

$$W_n = \omega_J[2\cos(k) + (-1)^n x]. \tag{28}$$

The resulting system of equations can best be understood when expressed in matrix form. Towards this end we define the $G$-component column matrices

$$\alpha_D = \begin{pmatrix} a_D^{\text{in}} \\ a_D^{\text{out}} \\ 0 \\ 0 \\ \vdots \\ 0 \end{pmatrix} \tag{29}$$

and

$$\alpha_S = \begin{pmatrix} a_S^{\text{in}} \\ a_S^{\text{out}} \\ 0 \\ 0 \\ \vdots \\ 0 \end{pmatrix} \tag{30}$$

and the $G$-component column matrix

$$\alpha_k = \begin{pmatrix} a_{k,1} \\ a_{k,2} \\ \vdots \\ a_{k,G} \end{pmatrix}. \tag{31}$$

We will also define the $G \times G$ square matrices $Q_D$ and $Q_S$ and the $G \times G$ matrices $M$ and $N$ such that

$$Q_D \alpha_D = M \alpha_k \tag{32}$$

and

$$N \alpha_k = Q_S \alpha_S. \tag{33}$$

Performing the aforementioned substitutions, we arrive at a system of equations such that these matrices are defined as

$$Q_D = \begin{pmatrix} e^{-iGK} & e^{iGk} & 0 & 0 & \cdots & 0 \\ e^{-i(G+1)k} & e^{i(G+1)k} & 0 & 0 & \cdots & 0 \\ 0 & 0 & 1 & 0 & \cdots & 0 \\ 0 & 0 & 0 & 1 & \cdots & 0 \\ \vdots & \vdots & \vdots & 0 & \ddots & \vdots \\ 0 & 0 & 0 & 0 & 0 & 1 \end{pmatrix}, \tag{34}$$

$$Q_S = \begin{pmatrix} e^{ik} & e^{-ik} & 0 & 0 & \cdots & 0 \\ 1 & 1 & 0 & 0 & \cdots & 0 \\ 0 & 0 & 1 & 0 & \cdots & 0 \\ 0 & 0 & 0 & 1 & \cdots & 0 \\ \vdots & \vdots & \vdots & 0 & \ddots & \vdots \\ 0 & 0 & 0 & 0 & 0 & 1 \end{pmatrix}, \tag{35}$$

$$M = \begin{pmatrix} 0 & \cdots & 0 & 0 & 0 & 0 & 0 & 1 \\ 0 & \cdots & 0 & 0 & 0 & 0 & -1 & W_G \\ 0 & \cdots & 0 & 0 & 0 & -1 & W_{G-1} & -1 \\ 0 & \cdots & 0 & 0 & -1 & W_{G-2} & -1 & 0 \\ \vdots & \cdots & 0 & \iddots & \iddots & \iddots & \cdots & 0 \\ -1 & W_2 & -1 & 0 & 0 & 0 & \cdots & 0 \end{pmatrix}, \tag{36}$$

and

$$N = \begin{pmatrix} 1 & 0 & 0 & 0 & 0 & \cdots & 0 \\ W_1 & -1 & 0 & 0 & 0 & \cdots & 0 \\ -1 & W_2 & -1 & 0 & 0 & \cdots & 0 \\ 0 & -1 & W_3 & -1 & 0 & \cdots & 0 \\ \vdots & \ddots & \ddots & \ddots & \ddots & \vdots & \vdots \\ 0 & 0 & 0 & 0 & -1 & W_{G-1} & -1 \end{pmatrix}, \tag{37}$$

From Eqs. (32) and (33) we see that

$$\alpha_D = \left(Q_D^{-1} M\right)(N^{-1} Q_S)\alpha_S. \tag{38}$$

The elements of the transfer matrix will be the upper $2 \times 2$ block of the matrix

$$T = \left(Q_D^{-1} M\right)(N^{-1} Q_S). \tag{39}$$

In order to calculate these matrix elements we must calculate the inverse matrices $Q_D^{-1}$ and $N^{-1}$.

### A. Matrix inverses

Since the matrix $Q_D$ is block diagonal, with a nonzero upper $2\times 2$ block and lower $(G-2)\times(G-2)$ block that equals the unity matrix, the inverse matrix can easily be found to be

$$Q_D^{-1}=\frac{1}{\delta_D}\begin{pmatrix} e^{i(G+1)k} & -e^{iGk} & 0 & 0 & \cdots & 0\\ -e^{-i(G+1)k} & e^{iGk} & 0 & 0 & \cdots & 0\\ 0 & 0 & 1 & 0 & \cdots & 0\\ 0 & 0 & 0 & 1 & \cdots & 0\\ \vdots & \vdots & \vdots & 0 & \ddots & \vdots\\ 0 & 0 & 0 & 0 & 0 & 1\end{pmatrix}, \tag{40}$$

where $\delta_D$ is the determinant of the upper $2\times 2$ block of the matrix $Q_D$:

$$\delta_D = 2i\sin(k). \tag{41}$$

Matrix $N$ is of rectangular tridiagonal form. According to Eq. (33), we wish to calculate the left-inverse matrix $N^{-1}$, which is a $G\times G$ matrix. Such inverses can be calculated using induction methods [18,19] such that each row of $N^{-1}$ is calculated recursively from each previous row. Since we only need the upper $2\times 2$ block of the matrix defined in Eq. (39), we only need the first two columns of the matrix $N^{-1}Q_S$, along with the first two rows of the matrix $Q_D^{-1}M$. From the matrices in Eqs. (36) and (40), the first two rows of $Q_D^{-1}M$ will be

$$\frac{1}{\delta_D}(0,\ldots,\quad 0,\quad e^{iGk},\quad e^{i(G+1)k}-W_G e^{iGk}) \tag{42}$$

and

$$\frac{1}{\delta_D}(0,\ldots,\quad 0,\quad -e^{-iGk},\quad -e^{-i(G+1)k}+W_G e^{-iGk}), \tag{43}$$

respectively. Note that only the last two elements are nonzero. Therefore, of the first two columns of $N^{-1}Q_S$, we only need the last two elements of each, meaning that of the matrix $N^{-1}$ we only need to calculate the rows $G-1$ and $G$. As a final simplification, since only the first two elements of the first two columns of the matrix $Q_S$ are nonzero, we conclude that, of the rows $G-1$ and $G$ of matrix $N^{-1}$, we only need to calculate the first two elements.

To summarize, the transfer matrix for the exciton transistor can be fully described by the lower left $2\times 2$ block of the matrix $N^{-1}$, meaning we only require the matrix elements $N^{-1}_{G-1,1}$, $N^{-1}_{G-1,2}$, $N^{-1}_{G,1}$, and $N^{-1}_{G,2}$. We find from our recursive calculations that, for the first column of $N^{-1}$,

$$N^{-1}_{2n+1,1}=\sum_{j=1}^{n+1}(-1)^{j-1}\binom{2n+1-j}{j-1}W_1^{n-j+1}W_2^{n-j+1} \tag{44}$$

and

$$N^{-1}_{2n,1}=\sum_{j=1}^{n}(-1)^{j-1}\binom{2n-j}{j-1}W_1^{n-j+1}W_2^{n-j}, \tag{45}$$

while for the second column of $N^{-1}$,

$$N^{-1}_{2n+1,2}=\sum_{j=1}^{n}(-1)^{j}\binom{2n-j}{j-1}W_1^{n-j}W_2^{n-j+1} \tag{46}$$

and

$$N^{-1}_{2n,2}=\sum_{j=1}^{n}(-1)^{j}\binom{2n-j-1}{j-1}W_1^{n-j}W_2^{n-j}, \tag{47}$$

where $\binom{y}{z}$ is the combination function $y$ choose $z$: $\binom{y}{z}=\frac{y!}{z!(y-z)!}$. From these we can calculate the required elements of the matrix $N^{-1}$.

### B. Transfer matrix

From the definition of the matrix $T$ in Eq. (39), the transfer matrix is

$$\begin{pmatrix}a_D^{\rm in}\\ a_D^{\rm out}\end{pmatrix}=\begin{pmatrix}T_{11} & T_{12}\\ T_{21} & T_{22}\end{pmatrix}\begin{pmatrix}a_S^{\rm in}\\ a_S^{\rm out}\end{pmatrix}. \tag{48}$$

Similarly constructed is the scattering matrix $S$, connecting the output transmitted waves from those input. It is

$$\begin{pmatrix}a_S^{\rm out}\\ a_D^{\rm out}\end{pmatrix}=\begin{pmatrix}S_{11} & S_{12}\\ S_{21} & S_{22}\end{pmatrix}\begin{pmatrix}a_S^{\rm in}\\ a_D^{\rm in}\end{pmatrix}. \tag{49}$$

Comparing these gives

$$S=T_{12}^{-1}\begin{pmatrix}-T_{11} & 1\\ -\det(T) & T_{22}\end{pmatrix}. \tag{50}$$

We identify the transmission coefficient as $t=T_{12}^{-1}$ and the transmission probability as

$$T=|t|^2=\frac{1}{|T_{12}|^2}. \tag{51}$$

We find, from the above,

$$\begin{aligned}T_{12}=\frac{e^{i(G+1)k}}{2i\sin(k)}\big\{&e^{-2ik}N^{-1}_{G-1,1}-[2\cos(k)\pm x]e^{-2ik}N^{-1}_{G,1}\\&+N^{-1}_{G,2}+e^{-ik}N^{-1}_{G-1,2}+e^{-ik}N^{-1}_{G,1}\\&-[2\cos(k)\pm x]e^{-ik}N^{-1}_{G,2}\big\},\end{aligned} \tag{52}$$

and given values of $k$ and $x$, we can use this expression to calculate the transmission probability

$$\begin{aligned}T^{-1}=\frac{\omega_J^2}{4\sin^2(k)}\big\{&\big(N^{-1}_{G-1,1}\big)^2+\big(N^{-1}_{G-1,2}\big)^2\\&+[1\pm 2x\cos(k)+x^2]\big[\big(N^{-1}_{G,1}\big)^2+\big(N^{-1}_{G,2}\big)^2\big]\\&+2\cos(k)[1\pm 2x\cos(k)+x^2]\big(N^{-1}_{G,1}N^{-1}_{G,2}\big)\\&-2[2\cos^2(k)-1\pm x\cos(k)]\big(N^{-1}_{G,1}N^{-1}_{G-1,2}\big)\\&-2[\cos(k)\pm x]\big(N^{-1}_{G-1,1}N^{-1}_{G,1}+N^{-1}_{G,2}N^{-1}_{G-1,2}\big)\\&-2[1\pm x\cos(k)]\big(N^{-1}_{G-1,1}N^{-1}_{G,2}\big)\\&+2\cos(k)\big(N^{-1}_{G-1,1}N^{-1}_{G-1,2}\big)\big\}.\end{aligned} \tag{53}$$

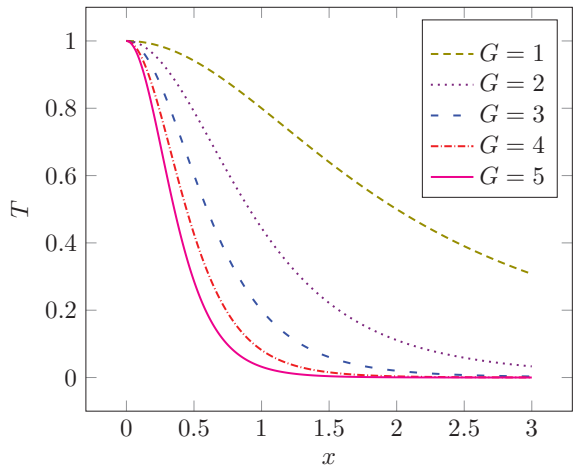


FIG. 2. Plot of the transmission probability $T$ versus the interaction strength $x = \frac{|\omega_K|}{|\omega_J|}$ for gate sizes $G$ ranging from $G = 1$ to 5. The transmission probability is the switching ratio of the exciton transistor device.

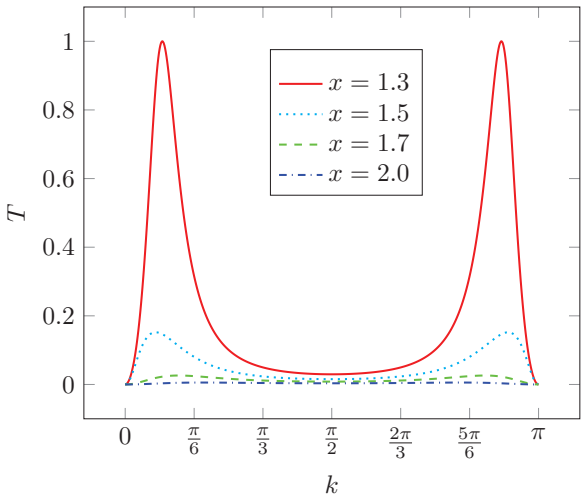


FIG. 3. Plot of the transmission probability $T$ versus the wave number $k$ for a gate size of $G = 4$.

This, along with Eqs. (44)–(47), is used to find the switching ratio of the exciton gate in the off state.

## VI. ANALYTICAL RESULTS

The switching ratio of the exciton transistor at midband is calculated from Eq. (53) with the wave number $k = \pi/2$. The results are plotted in Fig. 2. As expected, as $x$ increases we see the switching ratio improve, that is, largely denying excitonic passage to the drain since we are increasing the interaction strength between the gate molecule and the gate-channel molecules, thereby improving the Bragg grating and its band-gap effect.

For chromophores with difference static dipole strengths of $x > 1$, which are achievable [9], the analytical value of the transmission probability is given in Table I for a particular set of example values of $x$. In the application regime of scalable quantum computation, in order to implement quantum error correction, it is preferred that the gate errors not exceed one part in 100 [20,21]. We conclude that for an operational switchable gate, a control molecule engineered for a larger value of $x$ near $x = 2.0$ requires a gate size of $G \geqslant 4$ to achieve this error threshold. A gate size of $G = 5$ would naturally allow a smaller interaction strength, given these desired constraints.

In order to fully characterize the exciton transistor we also want to analyze the switching ratios over a range of exciton group velocities. For the desired gate sizes of $G = 4$ and 5, these results are shown in Figs. 3 and 4, respectively. Immediately noteworthy is that the fastest excitons are readily suppressed: They are essentially squelched for $G \geqslant 4$ over a wide range of difference static dipole interaction strengths. This is a result of an effective Bragg grating, which largely blocks signals with wavelengths near twice the periodicity of the grating.

We also recognize that for smaller interaction strength $x$ and at slow speeds, the system exhibits source-drain bleedthrough of excitons having de Broglie wavelengths not effectively blocked by the Bragg grating. This is not ideal behavior and greatly limits the bandwidth of the device. We therefore require this bleedthrough to be suppressed, which in turn requires increasing the difference static dipole-dipole interaction strength between the control molecule and the gate-channel molecules above a certain threshold. We can see from the values in Table II that, for a gate size of either four or five molecules, an interaction strength of $x = 2$ would

TABLE I. Transmission probability $T$ at midband, with $k = \pi/2$.

| | $T$ | | |
|---|---|---|---|
| $G$ | $x = 1.5$ | $x = 1.7$ | $x = 2$ |
| 1 | 0.640 | 0.581 | 0.500 |
| 2 | 0.221 | 0.167 | 0.111 |
| 3 | $6.06 \times 10^{-2}$ | $3.84 \times 10^{-2}$ | $2.00 \times 10^{-2}$ |
| 4 | $1.55 \times 10^{-2}$ | $8.33 \times 10^{-3}$ | $3.46 \times 10^{-3}$ |
| 5 | $3.40 \times 10^{-3}$ | $1.79 \times 10^{-3}$ | $5.95 \times 10^{-4}$ |

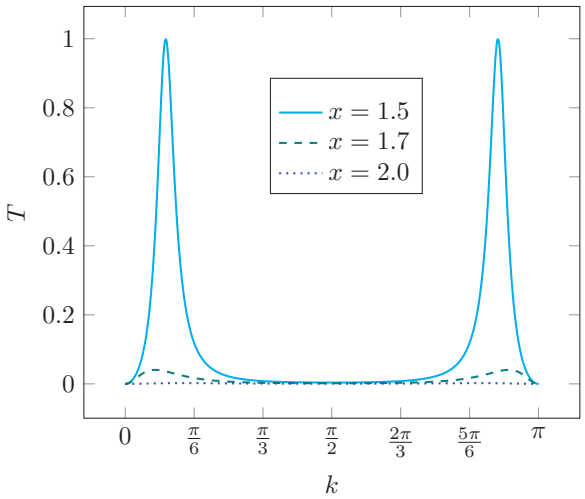


FIG. 4. Plot of the transmission probability $T$ versus the wave number $k$ for a gate size of $G = 5$.

TABLE II. Values for the local maxima of the transmission probabilities seen in Figs. 3 and 4.

| | $T_{\max}$ | | |
|---|---|---|---|
| $G$ | $x = 1.5$ | $x = 1.7$ | $x = 2$ |
| 4 | 0.152 | $2.61 \times 10^{-2}$ | $5.60 \times 10^{-3}$ |
| 5 | 1.0 | $4.06 \times 10^{-2}$ | $2.16 \times 10^{-3}$ |

allow us to achieve our desired performance over the entire bandwidth of the device. This conclusion is further demonstrated in Fig. 5, for which we can see that for $G = 4$ or 5, our switching ratio remains below the desired threshold over the entire device bandwidth for a gate-molecule–gate-channel molecule interaction strength of $x = 2$. The antennas which feed the excitons on the source side of the device can be tailored to couple to a specific wave number $k$ and polarization, allowing for control of the group velocity such that the device can operate in its ideal state.

## VII. CONCLUSION

In this paper we have demonstrated the viability of a simple, switchable exciton gate device. Its design enables on-off control through the excitation of a single controlling gate molecule. It interacts via a difference static dipole coupling with a number of nearby molecules comprising the gate channel. While the exciton gate is in the off state, the exciton propagating along the transmission-line–gate-channel system will transmit with a much reduced probability, and the exciton gate acts in this capacity as an off switch. Contrastingly, deexcitation of the control molecule uncouples it from the gate channel and incident excitons freely pass through, and the gate operates in the on-switch configuration.

Given the ideal operation of the device is for a small number of gate molecules $G = 4$ or 5, along with the fact that actual transmission lines feeding the gate will be short, decoherence effects due to noise is expected to be minimized, allowing the gate to operate as presented. Such exciton gates can be incorporated into quantum information processing systems as well as ultrafast switching applications. The interaction between an exciton of the gate molecule and the exciton propagating along the gate channel is nondissipative and therefore the gate can serve to create entangled superposition states.

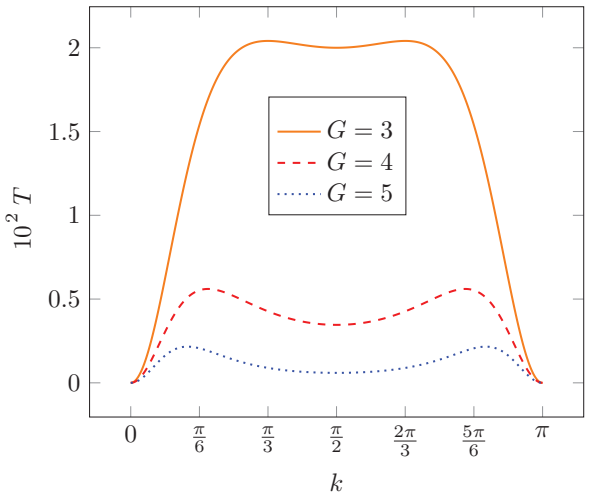


FIG. 5. Plot of the transmission probability $T$ versus the wave number $k$ for a gate-molecule–gate-channel molecule interaction strength of $x = 2$.

In order to maintain small gate errors, we have shown that an ideal exciton gate will have a gate size of no less than four chromophores, and the gate molecule should have a difference static dipole interaction strength between the gate molecules and the gate-channel molecules not significantly less than two times the hopping energy of the transmission lines. Organic dyes are attractive for the assembly of exciton gates with these coupling strengths, since such dyes can exhibit transition dipoles and difference static dipoles in the 10-D range [3,9,10]. Furthermore, the assembly of such dyes into transmission lines and other well-defined structures using DNA-based self-assembly techniques has received considerable attention [22]. We therefore conclude that the proposed scheme is a good candidate for a switching gate incorporated into quantum information processing systems.

A final note regards the means by which inputs can be fed into the gate and outputs delivered from the gate. It is essential that such dynamics takes place on a timescale that is fast compared to the decoherence time. This consideration is beyond the scope of the present paper, but an intriguing complication for these systems and for applications for quantum information processing. For optical switching applications, the interconversion of photons and excitons is desirable. Since the device presented here employs coherent interactions it is imperative that photons be transduced into excitons and injected into the device on a timescale that is fast compared to the dephasing time and that the conversion of the output excitons back into photons occurs on a similarly fast timescale. We suggest that requisite shortening of the radiative lifetime may be achievable with photon to exciton transducers that employ both superradiance [23] and Purcell cavity enhancement [24]. Such a device could be created by embedding a superradiant antenna array in an optical microcavity with small effective mode volume [25].

## ACKNOWLEDGMENTS

U.S. Department of Energy (DOE), Office of Basic Energy Sciences, Materials Sciences and Engineering Division and DOE's Established Program to Stimulate Competitive Research (EPSCOR) program via Award No. DE-SC0020089 for supporting the work concerning the foundational science aspects of quantum entanglement and the Department of the Navy, Office of Naval Research (ONR) under ONR Award No. N00014-19-1-2615 for supporting the work concerning the applied science aspects of exciton device physics.

[1] D. Abramavicius, B. Palmieri, and S. Mukamel, Extracting single and two-exciton couplings in photosynthetic complexes by coherent two-dimensional electronic spectra, Chem. Phys. **357**, 79 (2009).

[2] K. M. Duncan, H. M. Byers, M. E. Houdek, S. K. Roy, A. Biaggne, M. S. Barclay, L. K. Patten, J. S. Huff, D. L. Kellis, C. K. Wilson, J. Lee, P. H. Davis, O. A. Mass, L. Li, D. B. Turner, J. A. Hall, W. B. Knowlton, B. Yurke, and R. D. Pensack, Electronic structure and excited-state dynamics of DNA-templated monomers and aggregates of asymmetric polymethine dyes, J. Phys. Chem. A **127**, 4901 (2023).

[3] M. Ketteridge, A. Biaggne, R. Rau, G. Barcenas, O. A. Mass, W. B. Knowlton, B. Yurke, and L. Li, Effect of substituent location on the relationship between the transition dipole moments, difference static dipole, and hydrophobicity in squaraine dyes for quantum information devices, Molecules **28**, 2163 (2023).

[4] O. Kühn, V. Chernyak, and S. Mukamel, Two-exciton spectroscopy of photosynthetic antenna complexes: Collective oscillator analysis, J. Chem. Phys. **105**, 8586 (1996).

[5] A. Chakrabarti, A. Schmidt, V. Valencia, B. Fluegel, S. Mazumdar, N. Armstrong, and N. Peyghambarian, Evidence for exciton-exciton binding in a molecular aggregate, Phys. Rev. B **57**, R4206(R) (1998).

[6] A. M. Childs, D. Gosset, and Z. Webb, Universal computation by multiparticle quantum walk, Science **339**, 791 (2013).

[7] B. Yurke, R. Elliott, and A. Sup, Implementation of a Frenkel exciton-based controlled phase shifter, Phys. Rev. A **107**, 012603 (2023).

[8] B. Yurke, in *Visions of DNA Nanotechnology at 40 for the Next 40*, edited by N. Jonoska and E. Winfree (Springer, Berlin, 2023), pp. 125–169.

[9] D. Jacquemin, Excited-state dipole and quadrupole moments: TD-DFT versus CC2, J. Chem. Theory Comput. **12**, 3993 (2016).

[10] G. Barcenas, A. Biaggne, O. A. Mass, C. K. Wilson, O. M. Obukhova, O. S. Kolosova, A. L. Tatarets, E. Terpetsching, R. D. Pensack, J. Lee, W. B. Knowlton, B. Yurke, and L. Li, First-principle studies of substituent effects on squaraine dyes, RSC Adv. **11**, 19029 (2021).

[11] Y. Yonetani, Exciton quantum dynamics in the molecular logic gates for quantum computing, Chem. Phys. **570**, 111860 (2023).

[12] M. A. Castellanos and A. P. Willard, Designing excitonic circuits for the Deutsch-Jozsa algorithm: Mitigating fidelity loss by merging gate operations, Phys. Chem. Chem. Phys. **23**, 15196 (2021).

[13] M. A. Castellanos, A. Dodin, and A. P. Willard, On the design of molecular excitonic circuits for quantum computing: The universal quantum gates, Phys. Chem. Chem. Phys. **22**, 3048 (2020).

[14] N. P. Sawaya, D. Rappoport, D. P. Tabor, and A. Aspuru-Guzik, Excitonics: A set of gates for molecular exciton processing and signaling, ACS Nano **12**, 6410 (2018).

[15] R. J. Hudson, T. S. C. MacDonald, J. H. Cole, T. W. Schmidt, T. A. Smith, and D. R. McCamey, A framework for multiexcitonic logic, Nat. Rev. Chem. **8**, 136 (2024).

[16] H. Fidder, J. Knoester, and D. A. Wiersma, Superradiant emission and optical dephasing in J-aggregates, Chem. Phys. Lett. **171**, 529 (1990).

[17] B. Yurke and W. Kuang, Passive linear nanoscale optical and molecular electronics device synthesis from nanoparticles, Phys. Rev. A **81**, 033814 (2010).

[18] Y. Zhang, X. Song, and Y. Yang, in *Proceedings of the 36th Youth Academic Annual Conference of Chinese Association of Automation, Nanchang, 2021* (IEEE, Piscataway, 2021), pp. 13–19.

[19] C. M. Da Fonseca and J. Petronilho, Explicit inverses of some tridiagonal matrices, Linear Algebra Appl. **325**, 7 (2001).

[20] A. M. Stephens, Fault-tolerant thresholds for quantum error correction with the surface code, Phys. Rev. A **89**, 022321 (2014).

[21] A. G. Fowler, M. Mariantoni, J. M. Martinis, and A. N. Cleland, Surface codes: Towards practical large-scale quantum computation, Phys. Rev. A **86**, 032324 (2012).

[22] D. Mathur, S. A. Diaz, N. Hildebrandt, R. D. Pensack, B. Yurke, A. Biggne, L. Li, J. S. Melinger, M. G. Ancona, W. B. Knowlton, and I. L. Medintz, Pursuing excitonic energy transfer with programmable DNA-based optical breadboards, Chem. Soc. Rev. **52**, 7848 (2023).

[23] U. Barotov, D. H. T. Arachchi, M. D. Klein, J. Zhang, T. Šverko, and M. G. Bawendi, Excitons in a two-dimensional supramolecular assembly, Adv. Opt. Mater. **11**, 2201471 (2023).

[24] K. J. Vahala, Optical microcavities, Nature (London) **424**, 839 (2003).

[25] A. Gondarenko and M. Lipson, Low modal volume dipole-like dielectric slab resonator, Opt. Express **16**, 17689 (2008).